



1 Influence of three phases of El Niño-Southern Oscillation on daily 2 precipitation regimes in China

3 Aifeng Lv^{1,2}, Bo Qu^{1,2}, Shaofeng Jia¹ and Wenbin Zhu¹

4 ¹Key Laboratory of Water Cycle and Related Land Surface Processes, Institute of Geographic Sciences and Natural Resources
 5 Research, Chinese Academy of Sciences, Beijing 100101, China

6 ²University of Chinese Academy of Sciences, Beijing 100049, China;

7 *Correspondence to:* Bo Qu (geo_qb@163.com) and Aifeng Lv (lvaf@163.com)

8 Abstract

9 In this study, the impacts of the El Niño-Southern Oscillation (ENSO) on daily precipitation regimes in China are examined
 10 using data from 713 meteorological stations from 1960 to 2013. We discuss the annual precipitation, frequency and intensity
 11 of rainfall events, and precipitation extremes for three phases (Eastern Pacific El Niño (EP), Central Pacific El Niño (CP), and
 12 La Niña (LN)) of ENSO events in both ENSO developing and ENSO decaying years. A Mann–Whitney U test was applied to
 13 assess the significance of precipitation anomalies due to ENSO. Results indicated that the three phases each had a different
 14 impact on daily precipitation in China and that the impacts in ENSO developing and decaying years were significantly different.
 15 EP phases caused less precipitation in developing years but more precipitation in decaying years; LN phases caused a reverse
 16 pattern. The precipitation anomalies during CP phases were significantly different than those during EP phases and a clear
 17 pattern was found in decaying years across China, with positive anomalies over northern China and negative anomalies over
 18 southern China. ENSO events which altered the frequency and intensity of rainfall roughly paralleled anomalies in annual
 19 precipitation; in EP developing years, negative anomalies in both frequency and intensity of rainfall events resulted in less
 20 annual precipitation while in CP decaying years, negative anomalies in either frequency or intensity typically resulted in
 21 reduced annual precipitation. ENSO events triggered more extreme precipitation events. In EP and CP decaying years and in
 22 LN developing years, the number of very wet days (R95p), the maximum rainfall in one day (Rx1d), and the number of
 23 consecutive wet days (CWD) all increased, suggesting an increased risk of flooding. In addition, more dry spells (DS) occurred
 24 in EP developing years, suggesting an increased likelihood of droughts during this phase.

25 **Key words:** ENSO, daily precipitation, climate extremes, China

26 1 Introduction

27 The El Niño-Southern Oscillation (ENSO), a coupled ocean-atmosphere phenomenon in the tropical Pacific Ocean, exerts
 28 enormous influence on climate around the world (Zhou and Wu, 2010). Traditionally, ENSO events can be divided into a warm
 29 phase (El Niño) and a cool phase (La Niña) based on sea surface temperature (SST) anomalies. An El Niño produces warming
 30 SSTs in the Central and Eastern Pacific, while La Niña produces an anomalous westward shift in warm SSTs (Gershunov and



31 Barnett, 1998). Precipitation appears especially vulnerable to ENSO events over a range of spatio-temporal scales and therefore
32 has been the focus of many ENSO-related studies (Lü et al., 2011). Global annual rainfall drops significantly during El Niño
33 phases (Gong and Wang, 1999) and a wetter climate occurs in East Asia during El Niño winters due to a weaker than normal
34 winter monsoon (Wang et al., 2008), but these anomalies are generally reversed during La Niña phases.

35 Various studies also extensively document the teleconnections between ENSO and precipitation variation in China (Huang
36 and Wu, 1989; Lin and Yu, 1993; Gong and Wang, 1999; Zhou and Wu, 2010; Lü et al., 2011; Zhang et al., 2013; Ouyang et
37 al., 2014). Zhou and Wu (2010) found that El Niño phases induced anomalous southwesterly winds in winter along the
38 southeast coast of China, contributing to an increase in rainfall over southern China. In the summer after an El Niño, insufficient
39 rainfall occurs over the Yangtze River, while excessive rainfall occurs in North China (Lin and Yu, 1993). During La Niña
40 phases, annual precipitation anomalies are spatially opposite of those during El Niño phases in China (Ouyang et al., 2014).

41 As ENSO events progress over the winter and into the following summer they influence both the developing and decaying
42 phases of El Niño and La Niña (Ropelewski and Halpert, 1987; Lü et al., 2011). Huang and Wu (1989) reported that the
43 developing stage of an El Niño caused a weak subtropical high which resulted in flooding of the Yangtze River and Huaihe
44 River, but the subtropical high shifted northward during the decaying phase, resulting in an inverse rainfall anomaly. The
45 delayed response of climate variability to ENSO provides valuable information for making regional climate predictions (Lü et
46 al., 2011).

47 Until recently, most studies have focused on changes in annual or seasonal total precipitation related to ENSO rather than
48 changes in individual precipitation events, although possible shifts in characteristics of precipitation events, e.g. frequency and
49 intensity, have been highlighted in studies of global climate change (Fowler and Hennessy, 1995; Karl et al., 1995; Gong and
50 Wang, 2000). In China, it was reported that the number of annual rainfall days has decreased even though total annual
51 precipitation has changed little in the past few decades (Zhai et al., 2005). Precipitation intensity has also changed significantly,
52 especially across China (Qu et al., 2016), and as a result, drought and flood events occur more frequently (Zhang and Cong,
53 2014). Thus, separating out the impact of ENSO events on precipitation frequency and intensity is critical to understanding
54 ENSO-precipitation teleconnections in China.

55 ENSO events are also well-known for causing extreme hydrological events (Moss et al., 1994; Chiew and McMahon, 2002;
56 Veldkamp et al., 2015) such as floods (Mosley, 2000; Räsänen and Kumm, 2013; Ward et al., 2014) and droughts (Perez et
57 al., 2011; Zhang et al., 2015) which in turn cause broad-ranging socio-economic and environmental impacts. Various
58 approaches have been introduced to reveal these impacts at global and regional scales. For example, Ward et al. (2014)
59 examined peak daily discharge in river basins across the world to identify flood-vulnerable areas sensitive to ENSO. Perez et
60 al. (2011) modelled non-contiguous and contiguous drought areas to analyze spatio-temporal drought development. Water
61 storage is another index typically used to detect frequency and magnitude of droughts during ENSO events (Veldkamp et al.,



2015; Zhang et al., 2015). Although the link between hydrological extremes and ENSO is usually discussed in the context of the physical mechanisms that influence local precipitation (Zhang et al., 2015), direct precipitation indices such as the number of consecutive wet days and dry spells have rarely been addressed in these studies. Thus, our knowledge of how daily precipitation extremes respond to ENSO events is still very limited and requires a comprehensive set of precipitation indices that describe ENSO-induced precipitation extremes.

A number of recent studies suggest that a new type of El Niño may now exist that is different from the canonical El Niño (Ren and Jin, 2011). This new El Niño develops in regions of warming SSTs in the Pacific near the International Date Line (McPhaden et al., 2006) and has been called “Dateline El Niño” or “Central Pacific (CP) El Niño.” Studies have revealed that CP El Niño appears to induce climate anomalies around the globe that are distinctly different than those produced by the canonical Eastern Pacific (EP) El Niño (Yeh et al., 2009). In addition, CP El Niño has been occurring more frequently in recent decades (Yu and Kim, 2013). Despite a long-term focus on ENSO-climate teleconnections, relatively little attention has been paid to the impacts of the new CP El Niño in China.

The current study began with the observation that EP El Niño has occurred less frequently and that CP El Niño has occurred more frequently during the late twentieth century (Yeh et al., 2009). The main objectives of this work are to document (1) any changes in daily rainfall in China during three different phases of ENSO events; (2) the number and duration of precipitation extremes occurring in both ENSO developing and decaying years. We discuss the total precipitation anomaly, anomalies of precipitation frequency and intensity patterns, and changes in precipitation extremes, and propose possible mechanisms responsible for the various rainfall anomalies.

2 Materials and methods

In this study, we used daily values of climate data from Chinese surface stations compiled by the National Meteorological Center in China. This dataset comprises detailed spatial coverage of precipitation across China, but only 400 stations were operational in the 1950s (Xu et al., 2011). Non-climatic noise can complicate the accuracy of analyses of the dataset (Qu et al., 2016). Stations that experienced observation errors, missing values, or data homogeneity problems were omitted from analysis in this study, according to similar methods used by Qian and Lin (2005). Of the 819 meteorological stations across China, data from 713 were ultimately selected for analysis which covered the time period between 1960 and 2013 (Fig. 1). Precipitation indices were calculated based on daily observations at the stations (Table 1). Precipitation amount, intensity, and frequency were used to formulate precipitation characteristics. Four new indices were introduced and used to analyse precipitation extremes in this study.

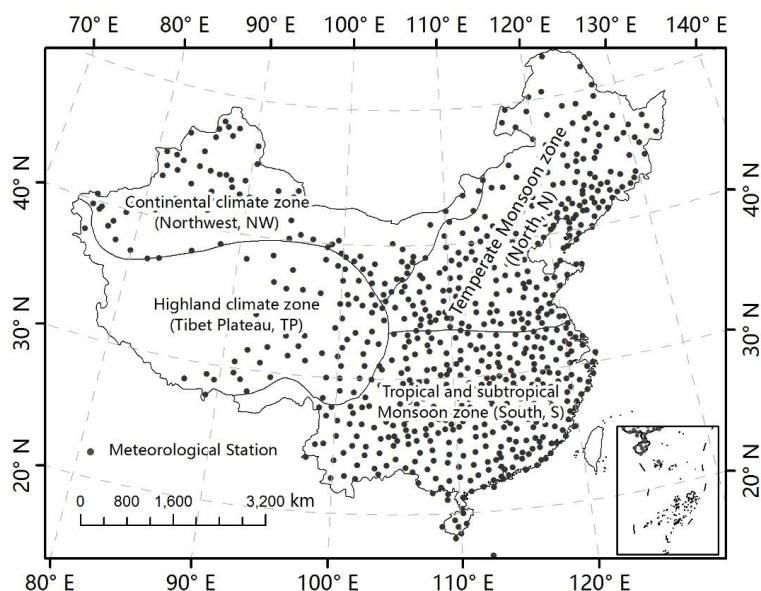


Fig. 1. The distribution of the 719 meteorological stations used in this study. China is divided into four regions based on main climatic types. The two non-monsoon regions are the continental climate zone (Northwest, NW) and the highland climate zone (Tibet Plateau, TP). The monsoon region is divided into two parts: the tropical and subtropical monsoon zone (South, S) and the temperate monsoon zone (North, N).

Table 1. Definitions of precipitation indices used in this study

Index	Descriptive name	Definition	Unit
P	Wet day precipitation	Annual total precipitation from wet days	mm
I	Simple daily intensity index	Average precipitation on wet days	mm/day
F	Number of wet days	Annual count of wet days	day
Rx1d	Maximum 1-day precipitation	Annual maximum 1-day precipitation	mm
R95p	Very wet day precipitation	Annual total precipitation when precipitation >95th percentile of multi-year average	mm
DS	dry spells	Number of consecutive dry days at least 10	-
CWD	consecutive wet days	Number of consecutive rainy days at least 3	-

In this study, two new indices created by Ren and Jin by transforming the traditionally-used Niño3 and Niño4 indices (2011) were used to distinguish between CP and EP El Niño phases. La Niña years were identified using the methods of McPhaden and Zhang (2009). The ENSO events (1960–2013) analyzed in this study are displayed in Table 2. Precipitation indices were calculated in both ENSO developing and decaying years. Indices for precipitation anomalies were analysed as follows:

$$A_{ij} = \frac{\overline{PI_{ij}} - \overline{PA_{ij}}}{\overline{PA_{ij}}} \quad (1)$$

Where $\overline{PI_{ij}}$ is the average of the i precipitation index in the j meteorological station in a specific time period, and $\overline{PA_{ij}}$ is the average of the i precipitation index in the j station in the multi-year average (represented by 1971–2000).



103

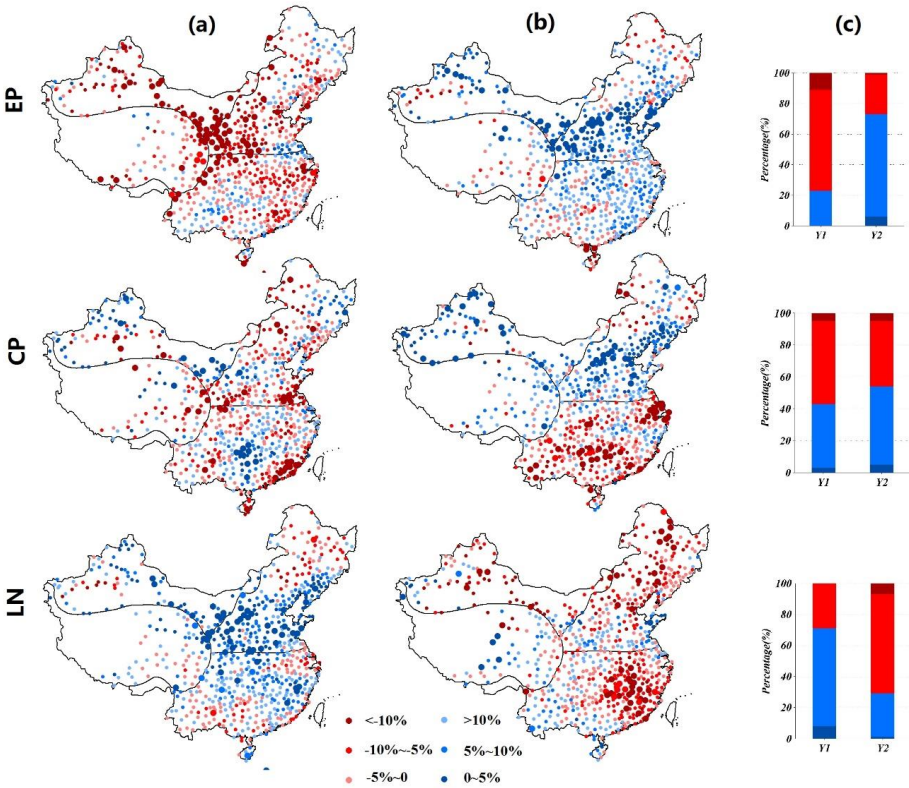
Table 2. ENSO years from 1960 to 2013

Phase	Eastern Pacific (EP)				Central Pacific (CP)				La Niña (LN)			
	El Niño				El Niño				La Niña (LN)			
	1963	1965	1969	1972	1968	1977	1987	1994	1964	1967	1970	1973
Year	1976	1982	1986	1991	2002	2004	2009		1975	1984	1988	1995
	1997	2006							1998	2007	2010	

104 The Mann–Whitney U test is a nonparametric test applied to site data that does not conform to normality even after several
 105 different transformations are carried out (Teegavarapu et al., 2013). This test was applied to evaluate the significance of
 106 precipitation anomalies, performing at a significance level of 5%.

107 3 Results

108 3.1 Annual rainfall anomalies

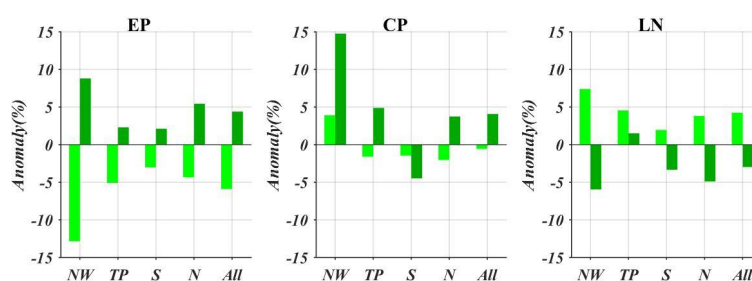


109

110 **Fig. 2** Anomalies of annual precipitation in developing years (a) and decaying years (b) of EP, CP, and LN phases. Stations
 111 experiencing significant anomalies are represented by large points. The percentage of stations experiencing increases or
 112 decreases in the number of rainfall anomalies are shown in (c), with significant increase (blue), increase (light blue), decrease
 113 (light red), and significant decrease (red). Y1, Y2 represent developing years and decaying years, respectively.



114 In EP developing years, 628 stations across China (~80%) had negative anomalies. At 80 of these stations the anomalies were
 115 significant. These significant stations were mainly located in the continental climate zone (NW) and the temperate monsoon
 116 zone (N) (Fig. 2). All sub-regions experienced negative average annual precipitation anomalies (Fig. 3), especially in the NW
 117 region where precipitation was 12.83% lower than the mean. Large positive anomalies of annual precipitation were found
 118 during LN developing years (Fig. 2); more than 70% of the stations showed positive anomalies, of which 10% were significant.
 119 Similarly, the stations with significant anomalies were mainly in the NW and N regions. In CP developing years, precipitation
 120 anomalies were quite different from those in EP developing years (Fig. 2). The proportion of stations with negative anomalies
 121 was 57%, but with no clear pattern of distribution.



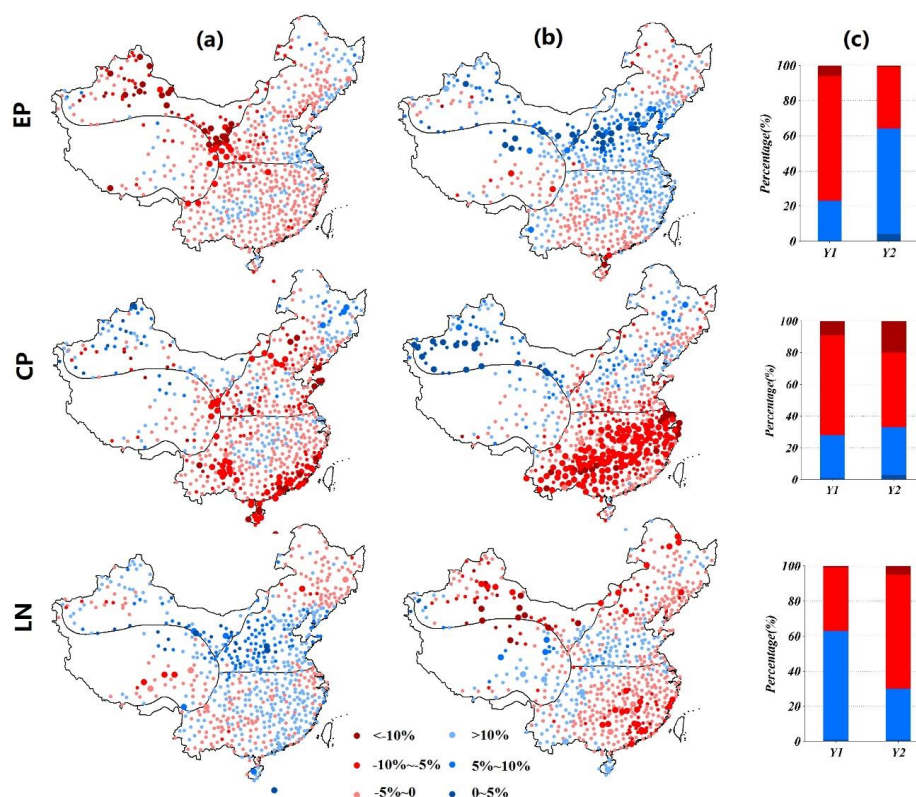
122

123 **Fig. 3** Average annual precipitation anomaly by sub-region during EP, CP, and LN phases. Light color represents developing
 124 years and dark color represents decaying years.

125 The impacts of EP phases on precipitation in decaying and developing years displayed opposite patterns. Positive anomalies
 126 were detected across China during decaying years (Fig. 2), especially in the NW and N regions at 8.8% and 8.9% higher than
 127 the mean, respectively (Fig. 3). And negative anomalies were common across China in LN decaying years (Fig. 2). In the NW
 128 region, average annual precipitation was 5.95% lower than the mean. As a result, in both the decaying years of EP and the
 129 developing years of LN, more water vapor would be transported from the Pacific Ocean to China, while in the decaying years
 130 of LN and the developing years of EP, drier conditions would prevail. In the CP phases, average annual precipitation in the
 131 NW, Tibet Plateau (TP), and N regions was much greater than the mean, but lower than the mean in the subtropical monsoon
 132 zone (S) (Fig. 3).

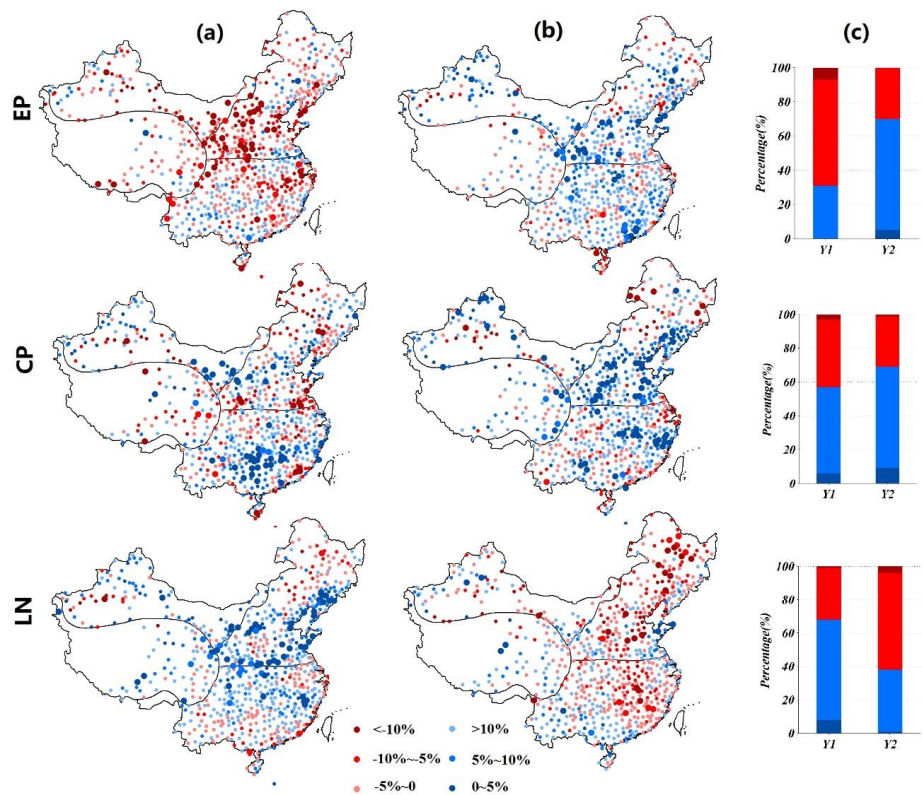


133 3.2 Rainfall frequency and intensity anomalies

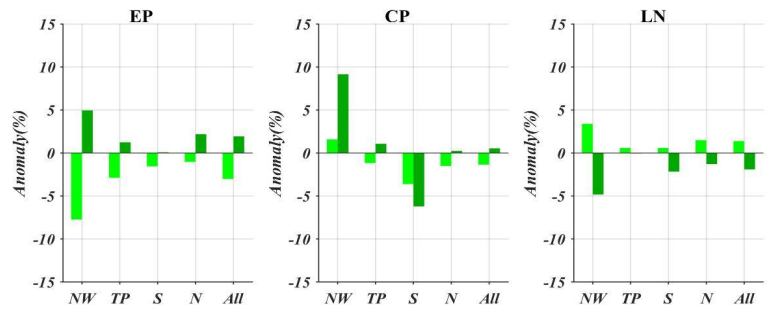


134
 135 **Fig. 4** Anomalies of precipitation frequency in developing years (a) and decaying years (b) of EP, CP, and LN phases. Stations
 136 experiencing significant anomalies are represented by large points. The percentage of stations experiencing anomalies of
 137 precipitation frequency are shown in (c), with significant increase (blue), increase (light blue), decrease (light red), and
 138 significant decrease (red). Y1, Y2 represent developing years and decaying years, respectively.

139



140
141 **Fig. 5** Anomalies of precipitation intensity in developing years (a) and decaying years (b) of EP, CP, and LN phases. Stations
142 experiencing significant anomalies are represented by large points. The percentage of stations experiencing anomalies of
143 precipitation frequency are shown in (c), with significant increase (blue), increase (light blue), decrease (light red), and
144 significant decrease (red). Y1, Y2 represent developing years and decaying years, respectively.



(a)

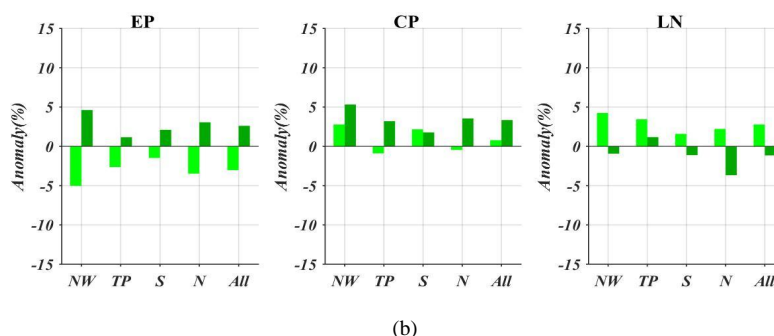


Fig. 6 Average anomalies of precipitation frequency (a) and precipitation intensity (b) by sub-region during EP, CP, and LN phases. Light color represents developing years and dark color represents decaying years.

In EP developing years, only negative anomalies of precipitation intensity and frequency occurred, with decreases of 3.04% and 3.01%, respectively, across all of China (Fig. 6). Stations with significant decreases in precipitation frequency were mainly located in the NW region (Fig. 4) and stations with significant decreases in precipitation intensity were mainly located in the N region (Fig. 5). In contrast, anomalies of precipitation intensity and frequency in EP decaying years were positive, presenting a reverse pattern to the developing phase. Anomalies of precipitation intensity and frequency were also positive in LN developing years, with stations of significance concentrated in the N region.

In the CP phases, anomalies of precipitation intensity and frequency displayed more complex patterns than those in the EP years. In developing years, slightly more than half of the stations experienced positive anomalies of precipitation intensity (Fig. 5), while more than 70% experienced negative anomalies in precipitation frequency. Of the stations experiencing negative precipitation frequency anomalies, 64 were significant (Fig. 4) and were concentrated in the S and N regions (Fig. 4). Precipitation frequency anomalies also formed a clear distribution pattern in CP decaying years. Of all the meteorological stations, 145 (20%) experienced significant negative anomalies and were concentrated in the S region. In contrast, all regions experienced positive anomalies of precipitation intensity.

In general, anomalies of total precipitation tend to result from changes in both the frequency and intensity of precipitation events. Combined with the analysis in section 3.1, the results suggest that increases in precipitation frequency and intensity during EP decaying years and LN developing years resulted in the positive anomalies of annual precipitation across China during these phases. And the decreases in precipitation frequency and intensity during EP developing years and LN decaying years resulted in the negative anomalies of annual precipitation. But, in the CP phases, few regions displayed such clear relationships between anomalies in total precipitation and precipitation events. For example, in the N region, precipitation frequency changed very little, and the observed positive anomalies of annual rainfall in CP decaying phases appear to have resulted from increased precipitation intensity. Likewise, in the S region, precipitation intensity increased by 1.77% even though the precipitation frequency and total precipitation decreased.



3.4 Precipitation extremes

ENSO can trigger extreme hydro-climatological events such as floods, droughts, and cyclones (Zhang et al., 2013). Table 3 shows the average percent change in the number of extreme precipitation events (anomalies of precipitation extremes) in sub-regions and the whole of China, based on data from all meteorological stations.

Table 3. Average anomalies of precipitation extremes during EP, CP, and LN phases (%).

Years	Phases	Index	NW	TP	S	N	All
Developing years	EP	Rx1d	-7.54	-2.23	-0.34	-0.32	-2.29
		R95p	-20.68	-7.02	-4.76	-5.55	-8.78
		DS	3.38	3.93	1.94	1.59	2.67
		CWD	-15.42	-6.07	-0.95	-3.70	-5.96
	CP	Rx1d	4.89	-1.00	1.02	-2.73	0.27
		R95p	5.79	-0.99	0.57	-2.93	0.28
		DS	-2.12	0.83	-0.10	2.18	0.34
		CWD	9.91	-2.11	-3.66	-3.33	-0.42
	LN	Rx1d	4.87	4.73	3.40	2.84	3.90
		R95p	10.79	8.90	4.76	8.10	7.97
		DS	-1.21	3.58	-0.25	0.26	0.71
		CWD	8.59	2.82	0.99	4.31	3.89
Decaying years	EP	Rx1d	9.52	1.30	2.43	1.94	3.43
		R95p	15.26	5.27	4.22	7.24	7.53
		DS	-3.83	1.70	0.26	1.76	0.21
		CWD	5.96	2.22	-1.48	6.72	3.18
	CP	Rx1d	7.54	4.36	2.39	0.28	3.39
		R95p	23.32	7.99	-0.33	7.13	8.64
		DS	4.08	-3.00	13.24	-1.88	3.05
		CWD	17.78	4.14	-4.78	1.11	3.71
	LN	Rx1d	-2.50	2.22	-1.00	-4.17	-1.29
		R95p	-4.73	2.14	-3.31	-9.06	-3.67
		DS	1.85	-2.48	1.35	0.87	0.30
		CWD	-7.86	-0.70	-1.81	-3.04	-3.06

During EP developing years and LN decaying years China experienced markedly negative anomalies in very wet daily rainfall, as expressed by the R95p index, and positive anomalies during EP decaying years and LN developing years. These impacts of the EP and LN phases on R95p were observed in nearly all sub-regions of China. An R95p positive anomaly was also observed in CP decaying years, but only in the NW, TP, and N regions. In CP developing years, the R95p identified no significant anomalies. The Rx1d index, a measure of maximum daily rainfall, revealed similar patterns to those identified by the R95p index. Positive R95p and Rx1d values during EP and CP decaying years and LN developing years indicate an increased likelihood of extreme precipitation events during these years than normal.

As shown in Table 3, negative anomalies of consecutive wet days (CWD) occurred in EP developing years and LN decaying years across China while the opposite pattern occurred in EP and CP decaying years and in LN developing years. The CWD



187 is a measure of wet conditions that is closely related to soil moisture and river runoff. A greater number of CWDs will enhance
188 soil moisture and increase runoff, but also increase the risk of floods. The NW region, a continental climate zone, is the most
189 sensitive of China's sub-regions to ENSO events in terms of CWDs. In EP developing years, the N, TP, and NW regions
190 experienced large decreases in CWDs (5.69%, 6.07%, and 15.42%, respectively). Such decreases have the potential to induce
191 droughts in these sub-regions as soil moisture decreases. But the dry conditions in these sub-regions reversed in EP decaying
192 years. Although a positive anomaly occurred in annual precipitation during CP decaying years in the N region, it nevertheless
193 experienced fewer CWD anomalies. This was possibly due to the increase in intensity of rainfall events.

194 Dry spells (DS) are extended periods of 10 days or more of no precipitation and are a strong predictor of droughts. As shown
195 in Table 3, all sub-regions of China experienced positive anomalies in DS during EP developing years, displaying an inverse
196 pattern to that observed for CWDs discussed above. In other words, fewer CWDs and more DS occurred simultaneously and
197 indicated an increased risk of drought. Negative anomalies in DS were observed in the NW and N regions during EP decaying
198 years. In CP decaying years, DS displayed dipole anomalies across China which were opposite of observed CWD patterns
199 during the same period. But during the same years, DS anomalies were positive in the NW region even though annual
200 precipitation had increased. DS displayed far weaker anomalies during both LN developing years and decaying years.

201 **4 Discussion and conclusion**

202 Using a nonparametric hypothesis test, this study investigated the impacts of three different ENSO phases on daily rainfall
203 regimes in China during the past half century. Rainfall data collected from meteorological stations across the country revealed
204 that the impacts of the three phases were significantly different from each other over both daily and annual time scales. In
205 addition, ENSO events triggered larger changes in both the frequency and intensity of precipitation events and the occurrence
206 of precipitation extremes than during non-ENSO periods. This finding is significant because past studies examining
207 teleconnections between ENSO events and climate variation in China have primarily focused on annual and/or monthly rainfall
208 rather than individual precipitation events. Since ENSO events can be predicted one to two years in advance using various
209 coupled ocean/atmosphere models (Lü et al., 2011), this study can provide a means of climate prediction on a daily time scale
210 and enable the prioritization of adaptation efforts ahead of extreme events.

211 The examination of variations in precipitation anomalies caused by different ENSO phases reveals a striking contrast between
212 the influences of canonical El Niño events (EP El Niño) and La Niña in China, which is consistent with previous studies on
213 global and regional scales (Ouyang et al., 2014; Veldkamp et al., 2015) and is due to opposite SST patterns over the central to
214 eastern Pacific Ocean. Namely, these SST patterns are positive in an EP El Niño phase and negative in a La Niña phase. In
215 contrast, during CP El Niño phases, precipitation over China displayed some asymmetric anomalies which do not follow the
216 patterns seen during either EP El Niño or La Niña years. For example, during CP decaying years, the N region experienced a



positive annual precipitation anomaly but a negative anomaly during La Niña decaying years. Meanwhile, the S region experienced a negative annual precipitation anomaly during the CP decaying phase. In addition, annual precipitation decreased notably during EP developing years, especially in the N and NW regions, but much less so during CP developing years. This incongruity between the influences of EP and CP El Niño phases reflects the potential for changes in atmospheric diabatic forcing over the tropics to modify tropical–midlatitude teleconnections to the El Niño (Yeh et al., 2009). When CP occurs, the evolution of the SST anomaly over tropical Pacific Ocean regions is significantly different than that which occurs during EP (Ashok et al., 2007); in other words, the magnitude of SST signals is not only weak during CP, but its position is also shifted westward, resulting in different atmospheric responses in the tropical Pacific Ocean. We also found that the S and NW regions are more sensitive to CP phases than other sub-regions of China in terms of precipitation events. In region S, for example, a remarkably negative anomaly in the frequency of precipitation events occurred during CP decaying years, resulting in a large increase in DS which partially explains the observed negative anomaly in annual precipitation. During the same years, the NW region displayed a strong positive anomaly in precipitation frequency which likely caused the sharp increase in annual precipitation, although the contribution of R95p cannot be ruled out as it was 23.32% greater than in no-ENSO years. Precipitation anomalies during the developing and decaying years of ENSO displayed inverse patterns as well. For example, a decrease in annual precipitation occurred across China during EP developing years, but an increase occurred during EP decaying years. Similar results were observed by Wu and Hu (2003) who documented seasonal rainfall anomalies in East Asia, finding that the rainfall correlation distribution displayed pronounced differences between developing and decaying ENSO years. This inverse relationship suggests a potential teleconnection between atmospheric responses in mid-latitude and the evolution of the SST anomaly over the tropical Pacific. During the developing stage, the warming SST anomaly of EP begins expanding during spring and reaches its maximum magnitude in autumn and winter (Feng et al., 2011). But during the following summer, during the ENSO decaying stage, the warming SST anomaly disappears and is replaced by a cool anomaly in the eastern Pacific. In contrast, the evolution of La Niña displays a reverse pattern that is supported by the same study which shows that the decaying and developing stages had opposite influences on rainfall over China. However, when CP phases occur, these inverse teleconnections seem to disappear. The CP decaying stage exerted a large influence on daily precipitation in China during decaying years, but in developing years it had little impact. The different teleconnections between EP and CP phases reflect differences in atmospheric responses to the evolution of the SST anomaly; CP phases progress more slowly and their peak state is of a shorter duration despite originating from a warmer background SST (Kim et al., 2009). It is important not to infer too much from only a few cases. As mentioned in Kim et al. (2009), it is hard to know whether the CP occurrence is part of a recurring natural cycle, like the Pacific multi-decadal oscillation, or the result of a warming climate. A possible origin of the physical processes causing changing precipitation regimes in China may be related to the evolution of the anomalous Western North Pacific (WNP) anti-cyclone and its direct influence on water vapor transport (Feng et al., 2011).



248 The frequency and intensity of precipitation events in China would change as a result. This study reveals that due to increased
249 WNP anti-cyclones during EP decaying phases, annual precipitation and the frequency and intensity of precipitation events
250 increased, especially in northern China. During CP developing years, the anomalous WNP anti-cyclone weakens and causes
251 no significant rainfall anomalies in China. However, during summer of CP decaying years, the WNP anti-cyclone re-
252 invigorates and extends north-westward toward inland regions (Wu et al., 2003). As a result, plentiful moisture is transported
253 to northern and northwestern China. Also, precipitation extremes may change in response to the different duration and
254 magnitude of precipitation events.

255 The climate of several regions in China are vulnerable to ENSO events via teleconnections, such as the South China Sea (Qu
256 et al., 2004; Rong et al., 2007; Zhou and Chan, 2007; Liu et al., 2011) and Yangzi River (Huang and Wu, 1989; Tong et al.,
257 2006; Zhang et al., 2007; Zhang et al., 2015). However, in this study, we found that the continental climate zone (NW) is more
258 sensitive to ENSO events than these and other regions based on the region's high incidence and magnitude of anomalies in
259 average annual precipitation. For example, the NW region experienced the largest anomalies in annual precipitation in China
260 during all phases of ENSO events. The NW region also demonstrated high sensitivity to the new type of El Niño, CP El Niño.

261 In an earlier study on daily river discharges at the global scale, Ward et al. (2014) found that ENSO has a greater impact on
262 annual floods in arid regions than non-arid regions, but suggested that the hydro-climatic response to ENSO in arid regions
263 has drawn much less attention than tropical regions. In China, Hui et al. (2006) analyzed the interdecadal variations in summer
264 rainfall in response to the SST anomaly over the Niño-3 region. They found that summer rainfall in northwestern China was
265 well-predicted by ENSO events between 1951–1974 (Hui et al., 2006). Over a longer period, Ouyang et al. (2014) found that
266 most parts of northwestern China experienced greater precipitation during El Niño months over the last century than during
267 non-El Niño months. But little work has been done on the mechanisms behind the climatic responses to ENSO events in the
268 continental climate zone of China, since most of studies have focused on monsoon zones (Matsumoto and Takahashi, 1999;
269 Wen et al., 2000; Wang et al., 2008; Zhou and Wu, 2010). Approaches to understanding the forces influencing daily
270 precipitation events coinciding with ENSO are more complex than those directed toward precipitation influences on a monthly
271 or annual scale. This complexity can be illustrated by the observation that in CP decaying years, the N region experienced a
272 positive anomaly of annual precipitation due to an increase in precipitation intensity, but the S region experienced a negative
273 anomaly due to a large decrease in precipitation frequency. And in terms of precipitation extremes, a new index, R95p, was
274 required to reveal an increase in precipitation intensity in the N region while the DS and CWD indices revealed anomalies in
275 the S region. Therefore, even though solid physics exists to explain precipitation variabilities related to ENSO events, there is
276 a need for more research on the mechanisms driving atmospheric circulation to advance our understanding of these influences
277 over time and spatial scales.



278 Finally, the year-to-year variability of the East Asian summer monsoon is likely also influenced by complex air–sea–land and
279 tropical–extratropical interactions in addition to ENSO events. These interactions may include Tibetan Plateau heating,
280 Eurasian snow cover, and polar ice coverage (Wang et al., 2000). Other factors that may simultaneously contribute to
281 precipitation anomalies in China during ENSO events include forces which generate large-scale circulation events that alter
282 the extension–retreat of the monsoon trough (Chen et al., 2006), tropical cyclones (Wang and Chan, 2002; Kim et al., 2011),
283 and vertical wind shear (Chia and Ropelewski, 2002).

284 *Acknowledgements.* This study was funded by the National Key Research and Development Program of China (Grant No.
285 2016YFC0401307) and the National Natural Science Foundation of China (Grant No. 41671026). We gratefully appreciate the editor and
286 anonymous reviewers for their constructive comments on improving the original manuscript.

287 References

- 288 Ashok, K., Behera, S. K., Rao, S. A., Weng, H., and Yamagata, T.: El Niño Modoki and its possible teleconnection, Journal
289 of Geophysical Research: Oceans, 112, 2007.
- 290 Chen, T.-C., Wang, S.-Y., and Yen, M.-C.: Interannual variation of the tropical cyclone activity over the western North Pacific,
291 Journal of Climate, 19, 5709–5720, 2006.
- 292 Chia, H. H., and Ropelewski, C.: The interannual variability in the genesis location of tropical cyclones in the northwest Pacific,
293 Journal of Climate, 15, 2934–2944, 2002.
- 294 Chiew, F. H. S., and McMahon, T. A.: Global ENSO–streamflow teleconnection, streamflow forecasting and interannual
295 variability, Hydrological Sciences Journal, 47, 505–522, 2002.
- 296 Feng, J., Chen, W., Tam, C. Y., and Zhou, W.: Different impacts of El Niño and El Niño Modoki on China rainfall in the
297 decaying phases, International Journal of Climatology, 31, 2091–2101, 2011.
- 298 Fowler, A., and Hennessy, K.: Potential impacts of global warming on the frequency and magnitude of heavy precipitation,
299 Natural Hazards, 11, 283–303, 1995.
- 300 Gershunov, A., and Barnett, T. P.: Interdecadal modulation of ENSO teleconnections, Bulletin of the American Meteorological
301 Society, 79, 2715–2725, 1998.
- 302 Gong, D.-Y., and Wang, S.-W.: Severe summer rainfall in China associated with enhanced global warming, Climate Research,
303 16, 51–59, 2000.
- 304 Gong, D., and Wang, S.: Impacts of ENSO on rainfall of global land and China, Chinese Science Bulletin, 44, 852–857, 1999.
- 305 Huang, R., and Wu, Y.: The influence of ENSO on the summer climate change in China and its mechanism, Advances in
306 Atmospheric Sciences, 6, 21–32, 1989.



- 307 Hui, G., Yongguang, W., and Jinhai, H.: Weakening significance of ENSO as a predictor of summer precipitation in China,
308 Geophysical research letters, 33, 2006.
- 309 Karl, T. R., Knight, R. W., and Plummer, N.: Trends in high-frequency climate variability in the twentieth century, Nature,
310 377, 217-220, 1995.
- 311 Kim, H.-M., Webster, P. J., and Curry, J. A.: Impact of shifting patterns of Pacific Ocean warming on North Atlantic tropical
312 cyclones, Science, 325, 77-80, 2009.
- 313 Kim, H.-M., Webster, P. J., and Curry, J. A.: Modulation of North Pacific tropical cyclone activity by three phases of ENSO,
314 Journal of Climate, 24, 1839-1849, 2011.
- 315 Lü, A., Jia, S., Zhu, W., Yan, H., Duan, S., and Yao, Z.: El Niño-Southern Oscillation and water resources in the headwaters
316 region of the Yellow River: links and potential for forecasting, Hydrology and Earth System Sciences, 15, 1273-1281, 2011.
- 317 Lin, X.-c., and Yu, S.-q.: El Nino and rainfall during the flood season (June-August) in China, Acta Meteorologica Sinica, 51,
318 434-441, 1993.
- 319 Liu, Q., Feng, M., and Wang, D.: ENSO-induced interannual variability in the southeastern South China Sea, Journal of
320 oceanography, 67, 127-133, 2011.
- 321 Matsumoto, J., and Takahashi, K.: Regional differences of daily rainfall characteristics in East Asian summer monsoon season,
322 Geographical review of Japan, Series B., 72, 193-201, 1999.
- 323 McPhaden, M. J., Zebiak, S. E., and Glantz, M. H.: ENSO as an integrating concept in earth science, science, 314, 1740-1745,
324 2006.
- 325 McPhaden, M. J., and Zhang, X.: Asymmetry in zonal phase propagation of ENSO sea surface temperature anomalies,
326 Geophysical Research Letters, 36, 2009.
- 327 Mosley, M. P.: Regional differences in the effects of El Niño and La Niña on low flows and floods, Hydrological Sciences
328 Journal, 45, 249-267, 2000.
- 329 Moss, M. E., Pearson, C. P., and McKerchar, A. I.: The Southern Oscillation index as a predictor of the probability of low
330 streamflows in New Zealand, Water Resources Research, 30, 2717-2723, 1994.
- 331 Ouyang, R., Liu, W., Fu, G., Liu, C., Hu, L., and Wang, H.: Linkages between ENSO/PDO signals and precipitation,
332 streamflow in China during the last 100 years, Hydrology and Earth System Sciences, 18, 3651-3661, 2014.
- 333 Perez, G. C., Van Huijgevoort, M., Voß, F., and Van Lanen, H.: On the spatio-temporal analysis of hydrological droughts from
334 global hydrological models, Hydrology and Earth System Sciences, 15, 2963-2978, 2011.
- 335 Qian, W., and Lin, X.: Regional trends in recent precipitation indices in China, Meteorology and Atmospheric Physics, 90,
336 193-207, 2005.



- 337 Qu, B., Lv, A., Jia, S., and Zhu, W.: Daily Precipitation Changes over Large River Basins in China, 1960–2013, *Water*, 8,
338 10.3390/w8050185, 2016.
- 339 Qu, T., Kim, Y. Y., Yaremchuk, M., Tozuka, T., Ishida, A., and Yamagata, T.: Can Luzon Strait transport play a role in
340 conveying the impact of ENSO to the South China Sea?, *Journal of Climate*, 17, 3644–3657, 2004.
- 341 Räsänen, T. A., and Kumm, M.: Spatiotemporal influences of ENSO on precipitation and flood pulse in the Mekong River
342 Basin, *Journal of Hydrology*, 476, 154–168, 2013.
- 343 Ren, H. L., and Jin, F. F.: Niño indices for two types of ENSO, *Geophysical Research Letters*, 38, 2011.
- 344 Rong, Z., Liu, Y., Zong, H., and Cheng, Y.: Interannual sea level variability in the South China Sea and its response to ENSO,
345 *Global and Planetary Change*, 55, 257–272, 2007.
- 346 Ropelewski, C. F., and Halpert, M. S.: Global and regional scale precipitation patterns associated with the El Niño/Southern
347 Oscillation, *Monthly weather review*, 115, 1606–1626, 1987.
- 348 Teegavarapu, R. S. V., Goly, A., and Obeysekera, J.: Influences of Atlantic multidecadal oscillation phases on spatial and
349 temporal variability of regional precipitation extremes, *Journal of Hydrology*, 495, 74–93, 2013.
- 350 Tong, J., Qiang, Z., Deming, Z., and Yijun, W.: Yangtze floods and droughts (China) and teleconnections with ENSO activities
351 (1470–2003), *Quaternary International*, 144, 29–37, 2006.
- 352 Veldkamp, T. I., Eisner, S., Wada, Y., Aerts, J. C., and Ward, P. J.: Sensitivity of water scarcity events to ENSO-driven climate
353 variability at the global scale, *Hydrology and Earth System Sciences*, 19, 4081, 2015.
- 354 Wang, B., Wu, R., and Fu, X.: Pacific-East Asian teleconnection: how does ENSO affect East Asian climate?, *Journal of*
355 *Climate*, 13, 1517–1536, 2000.
- 356 Wang, B., and Chan, J. C.: How strong ENSO events affect tropical storm activity over the western North Pacific*, *Journal of*
357 *Climate*, 15, 1643–1658, 2002.
- 358 Wang, L., Chen, W., and Huang, R.: Interdecadal modulation of PDO on the impact of ENSO on the East Asian winter
359 monsoon, *Geophysical Research Letters*, 35, 2008.
- 360 Ward, P. J., Eisner, S., Flörke, M., Dettinger, M. D., and Kumm, M.: Annual flood sensitivities to El Niño–Southern
361 Oscillation at the global scale, *Hydrology and Earth System Sciences*, 18, 47–66, 2014.
- 362 Wen, C., Graf, H.-F., and Ronghui, H.: The interannual variability of East Asian winter monsoon and its relation to the summer
363 monsoon, *Advances in Atmospheric Sciences*, 17, 48–60, 2000.
- 364 Wu, R., Hu, Z.-Z., and Kirtman, B. P.: Evolution of ENSO-related rainfall anomalies in East Asia, *Journal of Climate*, 16,
365 3742–3758, 2003.
- 366 Xu, X., Du, Y., Tang, J., and Wang, Y.: Variations of temperature and precipitation extremes in recent two decades over China,
367 *Atmospheric Research*, 101, 143–154, 2011.



- 368 Yeh, S.-W., Kug, J.-S., Dewitte, B., Kwon, M.-H., Kirtman, B. P., and Jin, F.-F.: El Niño in a changing climate, *Nature*, 461,
369 511-514, 2009.
- 370 Yu, J. Y., and Kim, S. T.: Identifying the types of major El Niño events since 1870, *International journal of climatology*, 33,
371 2105-2112, 2013.
- 372 Zhai, P., Zhang, X., Wan, H., and Pan, X.: Trends in total precipitation and frequency of daily precipitation extremes over
373 China, *Journal of climate*, 18, 1096-1108, 2005.
- 374 Zhang, Q., Xu, C.-y., Jiang, T., and Wu, Y.: Possible influence of ENSO on annual maximum streamflow of the Yangtze River,
375 China, *Journal of Hydrology*, 333, 265-274, 2007.
- 376 Zhang, Q., Li, J., Singh, V. P., Xu, C. Y., and Deng, J.: Influence of ENSO on precipitation in the East River basin, South
377 China, *Journal of Geophysical Research: Atmospheres*, 118, 2207-2219, 2013.
- 378 Zhang, X., and Cong, Z.: Trends of precipitation intensity and frequency in hydrological regions of China from 1956 to 2005,
379 *Global and Planetary Change*, 117, 40-51, 2014.
- 380 Zhang, Z., Chao, B., Chen, J., and Wilson, C.: Terrestrial water storage anomalies of Yangtze River Basin droughts observed
381 by GRACE and connections with ENSO, *Global and Planetary Change*, 126, 35-45, 2015.
- 382 Zhou, L. T., and Wu, R.: Respective impacts of the East Asian winter monsoon and ENSO on winter rainfall in China, *Journal*
383 *of Geophysical Research: Atmospheres*, 115, 2010.
- 384 Zhou, W., and Chan, J. C.: ENSO and the South China Sea summer monsoon onset, *International Journal of Climatology*, 27,
385 157-167, 2007.